Transient Analysis of Multiple-Tuned Injection-Locked Amplifiers with Modulated Input Signal

ENRICO F. CALANDRA, MEMBER, IEEE, AND ANTONINO M. SOMMARIVA

Abstract—**A method for the dynamical investigation of reflection-type injection-locked amplifiers (ILA's) driven by modulated input signals is presented. Its distinctive feature is to cover the large-signal analysis of high-order ILA's, which allows the exploitation of broad-banding multiresonant structures. Small-parameter, stroboscopic, and congruence algebra techniques are combined in order to permit the calculation of output voltage transients directly in terms of amplitude and phase of the complex envelope, thus limiting the computational time required in CAD applications. Further, owing to the employed black-box (scattering matrix) description of the tank and coupling two-port, both linear and nonlinear subsystem identification can be performed in terms of measured data. As an example of the application of the method, a fourth-order ILA is analyzed, and results pertaining to BPSK modulated input signals are presented.**

I. INTRODUCTION

INJECTION synchronization of solid-state microwave oscillators received considerable attention in the last decades, from both experimental and theoretical points of view [1]–[5], [9]–[20]. In particular, an established application of this technique is the high-power amplification of low-phase-noise monochromatic or modulated signals at high microwave and millimeter-wave frequencies.

The design and optimization of such systems require having at one's disposal efficient and reliable analysis tools capable of predicting the dynamical behavior of the injection-locked amplifier (ILA) in response to a stationary or modulated sinusoidal input signal. In this connection, however, it is to be noted that adequate theories are available in the literature (for both low- and high-level injection) only in case of single-tuned circuits [6]–[14]. In fact, the investigation of multiple-tuned systems has been so far attacked [15]–[18] by resorting to a first-order expansion of the dynamic immittance introduced by Kurokawa in [15], which was subsequently acknowledged by the same author to become a poor approximation when large-signal operation is involved [19]. On the other hand, the use of the unabridged expression of the dynamic immittance is not satisfactory either, as already shown in [20] with reference to the locking stability investigation. This intrinsic inadequacy of the dynamic immittance approach can be explained by considering that it rests on a perturbed frequency concept which leads to modeling any high-order system by means of a pair of differential equations in the first derivatives of the oscillation complex envelope components, thus improperly reducing the number of degrees of freedom.

In this paper, a method is presented which, overcoming the aforementioned limitation, allows the large-signal analysis of the steady-state and transient behavior of high-order ILA's driven by amplitude and/or angle modulated input signals. The system model consists of a parallel *RC* nonlinear element connected to the input–output isolation circulator by means of a linear tank and coupling two-port which can include multiple-tuned resonators, thus permitting the investigation of broad-banding ladder structures such as the ones suggested in [15]. The proposed approach involves a two-step procedure. First, by combining small-parameter and stroboscopic techniques, a pair of differential equations (both of order one half of the system degree) in the amplitude and phase of the voltage at the diode wafer plane is derived (Section II). Then, by applying polynomial congruence algebra to the scattering-matrix description of the linear subsystem, the explicit dynamic transfer relationship which expresses the load voltage complex envelope as a function of input and wafer voltage phasors (and their derivatives) is obtained (Section III). In Section IV, the method is applied to determine the general equations concerning the case of ILA's with a parabolic (conductive and susceptive) nonlinearity and a Γ-type double-tuned resonant and coupling two-port. Finally, in order to show the suitability of the approach devised to practical CAD applications, some results pertaining to the computer simulation of the above system response to BPSK modulated signals are reported in Section V.

II. DIFFERENTIAL EQUATIONS AT DIODE WAFER PLANE

Since the class of microwave ILA's considered here obeys specific constraints for quasi-sinusoidal behavior under steady-state and transient operation (see below), our analysis will refer directly to the first harmonic equivalent circuit shown in Fig. 1. There, the active device is modeled

Manuscript received January 15, 1988; revised November 14, 1988. This work was supported by the Italian Ministero della Pubblica Istruzione.

The authors are with the Dipartimento di Ingegneria Elettrica, Universitá di Palermo, Viale delle Scienze, 90128 Palermo, Italy.

IEEE Log Number 8926581.

0018-9480/89/0500-0826$01.00 ©1989 IEEE

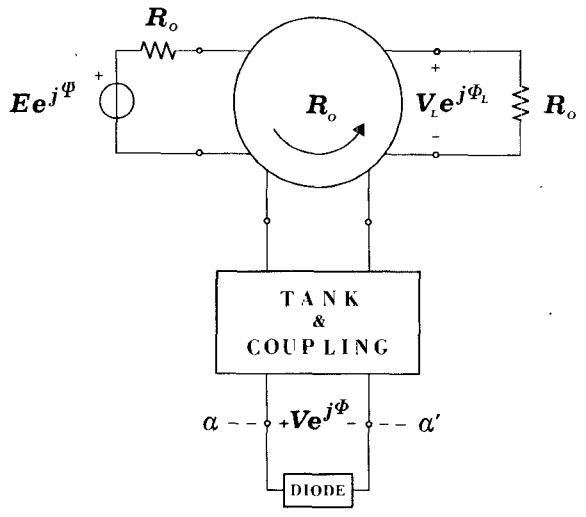

Fig. 1. First harmonic equivalent circuit of an injection-locked amplifier.

through a voltage-dependent admittance of the form

$$Y_d(V) = G_d(V) + j\omega C_d(V) \tag{1}$$

which accounts for both nonlinear conductance and susceptance effects at the diode wafer plane, and is easily obtainable through conventional large-signal measurement techniques [21]. As far as the tank and coupling circuit is concerned, we assume it to be a linear lumped time-invariant passive two-port characterized by means of its scattering matrix (calculated or measured). The input signal is supposed to be an amplitude- and/or angle-modulated sinusoid with carrier frequency (ω) near the free-running oscillation one (ω_o), and is injected through an input–output isolation circulator. For the sake of simplicity, the circulator is considered lossless and matched, as well as the source and load terminations, to the normalization resistance R_0. However, only minor changes to the treatment are required in order to remove these last assumptions.

The analysis of the output voltage dynamics of the circuit of Fig. 1 will be developed in two steps:

a) derivation of the differential nonlinear equations in the complex envelope components V and ϕ of the wafer voltage (this section);
b) derivation of the dynamic transfer relationship from wafer to load voltage (next section).

This two-step approach is proposed since for the class of circuits considered no general method can be developed for obtaining a set of differential equations directly in terms of the load voltage amplitude and phase. Moreover, in the few particular cases where such equations can be written, they are very involved and, therefore, hardly manageable with success.

To start with our calculations, the nonlinear steady-state equation at the wafer plane under CW operation is first derived. In this connection, it is convenient to separate the diode admittance $Y_d(V)$ into its linear ($Y_l = G_l + j\omega C_l$) and nonlinear ($Y_n(V) = G_n(V) + j\omega C_n(V)$) parts, and to

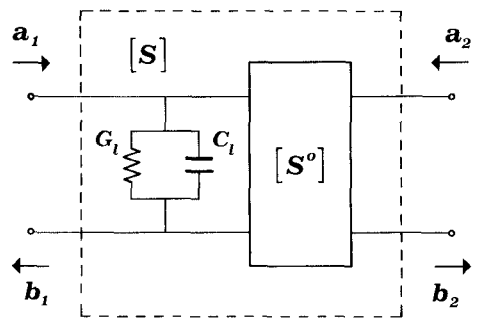

Fig. 2. Augmented tank and coupling two-port.

include the former in the tank and coupling circuit (see Fig. 2), introducing the overall wave quantities (a_i and b_i) and scattering parameters (S_{ij}) of the linear subsystem:

$$S_{11} = \frac{2S_{11}^0 - (1 + S_{11}^0)R_0Y_l}{2 + (1 + S_{11}^0)R_0Y_l}$$

$$S_{12} = S_{21} = \frac{2S_{12}^0}{2 + (1 + S_{11}^0)R_0Y_l}$$

$$S_{22} = \frac{2S_{22}^0 + (S_{22}^0 + \det[S^0])R_0Y_l}{2 + (1 + S_{11}^0)R_0Y_l}. \tag{2}$$

On the strength of the above definitions, we can write

$$b_1 - S_{11}a_1 = S_{12}a_2 \qquad a_2 = \frac{Ee^{j\Psi}}{2\sqrt{R_0}} \tag{3}$$

and

$$a_1 = (1 - R_0Y_n)\frac{Ve^{j\Phi}}{2\sqrt{R_0}} \qquad b_1 = (1 + R_0Y_n)\frac{Ve^{j\Phi}}{2\sqrt{R_0}} \tag{4}$$

with latter two being derived from

$$\frac{a_1}{b_1} = \frac{1 - R_0Y_n}{1 + R_0Y_n} \qquad Ve^{j\Phi} = (a_1 + b_1)\sqrt{R_0}. \tag{5}$$

By combining (3) and (4) we obtain the nonlinear phasor equation

$$[1 + R_0Y_n - S_{11}(1 - R_0Y_n)]Ve^{j\Phi} = S_{12}Ee^{j\Psi} \tag{6}$$

which provides the CW voltage amplitude and phase at the diode wafer plane.

With the view of deriving correct dynamic equations, it is necessary now to perform a narrow-band approximation of (6) around the free-running oscillation frequency ω_o, which avoids the improper doubling of the system degree and, therefore, the generation of spurious transient modes [22], [23]. To this end, we first express the scattering parameters as a ratio of polynomials of the form

$$S_{ij} = \frac{s_{ij}}{\Delta} = \frac{\sum_0^M (\omega^2 - \omega_o^2)^m (s'_{ij,m} + j\omega s''_{ij,m})}{\sum_0^M (\omega^2 - \omega_o^2)^m (\Delta'_m + j\omega\Delta''_m)} \tag{7}$$

(which can easily be done through formulas provided in

Appendix I), and then make use of the frequency truncations $(\omega^2-\omega_o^2)^m \doteq [2\omega_o(\omega-\omega_o)]^m$; $j\omega \doteq j\omega_o$. We then substitute into (6), for the quantities Y_n and S_{ij}, their abridged counterparts

$$\bar{Y}_n = G_n(V) + j\omega_0 C_n(V)$$

$$\bar{S}_{ij} = \frac{\bar{s}_{ij}}{\bar{\Delta}} = \frac{\sum_0^M (2\omega_o)^m(\omega-\omega_o)^m\left(s'_{ij,m}+j\omega_o s''_{ij,m}\right)}{\sum_0^M (2\omega_o)^m(\omega-\omega_o)^m\left(\Delta'_m+j\omega_0\Delta''_m\right)}. \quad (8)$$

We are now in a position to state the analytical conditions that guarantee quasi-sinusoidal quasi-static behavior under transient operation. This check is indeed necessary in the case of high-order systems, because one can rarely infer such characteristics on the basis of qualitative considerations only. Using the symbology implicitly introduced in (7), the constraints to be satisfied read

$$s''_{11,M} = \Delta''_M = 0 \quad (9a)$$

$$\left|1+\frac{s'_{11,M}}{\Delta'_M}\right| \ll 1 \quad (9b)$$

$$2\omega_o^2 \sqrt[M-m]{\frac{|s'_{11,M}|}{|s'_{ij,m}+j\omega_o s''_{ij,m}|}} \gg 1$$

$$2\omega_o^2 \sqrt[M-m]{\frac{|\Delta'_M|}{|\Delta'_m+j\omega_o\Delta''_m|}} \gg 1. \quad \{m<M\} \quad (9c)$$

The first condition corresponds to considering even order circuits, which implies, in this context, the absence of aperiodic dc-drifting modes. The second one accounts for the presence of a low-impedance shunt path for the current harmonics out of the active element, as needed for the suppression of voltage harmonics at the wafer plane. The third constraint extends to higher order systems the high-Q resonance requirement typical of second-order weakly nonlinear oscillators, by imposing proper scaling of the coefficients $s^{(\cdot)}_{ij,m}$, $\Delta^{(\cdot)}_m$. In this connection, let us observe that in the case where analytical expressions for such coefficients are available, a certain simplification of the calculations can be achieved by discarding from each $s^{(\cdot)}_{ij,m}$ and $\Delta^{(\cdot)}_m$ the terms of magnitude order less than the one implied by (9c) (see for instance the example worked out in Section IV).

Owing to the above-stated conditions and to the assumptions on the input signal bandwidth, all port voltages are accurately described under transient operation by phasors with slowly varying amplitude and phase. This allows us to obtain the dynamic equations at the wafer plane by rewriting (6) in the form

$$\left[\bar{\Delta}-\bar{s}_{11}+\left(\bar{\Delta}+\bar{s}_{11}\right)R_0\bar{Y}_n\right]Ve^{j\Phi} = \bar{s}_{12}Ee^{j\Psi} \quad (10)$$

and then replacing in it the operator $(\omega-\omega_o-jd/dt)^m$ for the quantity $(\omega-\omega_o)^m$, where the symbolic nth power of d/dt indicate nth-order time differentiation of the argument. After expansion, we therefore obtain the complex relationship

$$\sum_0^M \frac{(-j)^m}{m!}\frac{d^m\left(\bar{\Delta}-\bar{s}_{11}\right)}{d\omega^m}\frac{d^m\left(Ve^{j\Phi}\right)}{dt^m} + R_0\sum_0^{M-1}\frac{(-j)^m}{m!}\frac{d^m\left(\bar{\Delta}+\bar{s}_{11}\right)}{d\omega^m}\frac{d^m\left(\bar{Y}_nVe^{j\Phi}\right)}{dt^m} = \sum_0^M \frac{(-j)^m}{m!}\frac{d^m(\bar{s}_{12})}{d\omega^m}\frac{d^m(Ee^{j\Psi})}{dt^m}. \quad (11)$$

It is easily verified that the real and imaginary parts of (11) can always be solved for the maximum order derivatives of $V(t)$ and $\phi(t)$, thus providing a set of differential equations of the form

$$\frac{d^MV}{dt^M} = f\left(\frac{d^{M-1}V}{dt^{M-1}},\cdots,V;\frac{d^{M-1}\phi}{dt^{M-1}},\cdots,\phi;t\right)$$

$$\frac{d^M\phi}{dt^M} = g\left(\frac{d^{M-1}V}{dt^{M-1}},\cdots,V;\frac{d^{M-1}\phi}{dt^{M-1}},\cdots,\phi;t\right). \quad (12)$$

Once the actual input modulation waveforms are specified, numerical integration of (12) allows straightforward evaluation of amplitude and phase transients at the wafer plane, which accomplishes the first step of our procedure. As a final remark, let us notice that equations (12) are also in a form suitable for deriving the CW locking stability criteria through conventional linearization techniques [24]. Relevant formulations are provided in Appendix II.

III. Wafer-to-Load Dynamic Transfer Relationship

To calculate the amplitude and phase transients at the load plane, we take advantage of the fact that basic circuit theory ensures (regardless of the topology of the tank circuit) the existence of a phasor relationship between wafer, input, and output voltages of the form

$$V_Le^{j\Phi_L} = \left[p(j\omega)+q(j\omega)R_0Y_n\right]Ve^{j\Phi}+r(j\omega)Ee^{j\Psi} \quad (13)$$

$p(j\omega)$, $q(j\omega)$, and $r(j\omega)$ being polynomials of the argument $j\omega$. Indeed, the other possible alternative (i.e., calculating the load voltage complex envelope through the dynamic transfer function technique suggested in [17]) is not practicable, because it makes use of the perturbed frequency concept [15], whose inadequacy has been already pointed out in the Introduction.

Equation (13) could be obtained after applying a proper elimination algorithm to the set of equations describing the linear subnetwork. However, since only a scattering matrix description of the tank and coupling two-port is assumed here to be available, i.e., no knowledge of its actual topology is required, a different approach will be employed for the determination of $p(j\omega)$, $q(j\omega)$, and $r(j\omega)$. In particular, use will be made of the algebra of polynomial congruences [25], which also offers the advantage of a straightforward computer implementation.

As a first step, substituting into (13) the relationships

$$V_L e^{j\Phi_L} = b_2\sqrt{R_0} \qquad Ve^{j\phi} = (a_1 + b_1)\sqrt{R_0}$$
$$R_0 Y_n V e^{j\Phi} = (b_1 - a_1)\sqrt{R_0} \qquad Ee^{j\psi} = 2a_2\sqrt{R_0} \quad (14)$$

we obtain

$$b_2 = (p-q)a_1 + (p+q)b_1 + 2ra_2. \quad (15)$$

Substituting $S_{11}a_1 + S_{12}a_2$ for b_1 in (15) yields

$$b_2 = [p - q + S_{11}(p+q)]a_1 + [2r + S_{12}(p+q)]a_2. \quad (16)$$

By equating (16) with $b_2 = S_{21}a_1 + S_{22}a_2$, we obtain the set of equations

$$(S_{11}+1)p + (S_{11}-1)q = S_{21}$$
$$S_{12}p + S_{12}q = S_{22} - 2r \quad (17)$$

which, solved for p and q, provides

$$p = \frac{(1-S_{11})(S_{22}-2r) + S_{12}S_{21}}{2S_{12}}$$
$$q = \frac{(1+S_{11})(S_{22}-2r) - S_{12}S_{21}}{2S_{12}}. \quad (18)$$

Since p and q are known *a priori* to be polynomials, equations (18) imply the following set of congruences:

$$2\Delta(\Delta - s_{11})r \equiv (\Delta - s_{11})s_{22} + s_{12}s_{21} \quad [\text{mod } s_{12}]$$
$$2\Delta(\Delta + s_{11})r \equiv (\Delta + s_{11})s_{22} - s_{12}s_{21} \quad [\text{mod } s_{12}] \quad (19)$$

which, being certainly compatible, can be replaced by the simpler (equivalent) single congruence

$$2\Delta r \equiv s_{22} \quad [\text{mod } s_{12}]. \quad (20)$$

Once (20) is solved for r (see Appendix III), from (18) the polynomials p and q are easily determined. Through a narrow-banding technique analogous to the one followed in Section II, the truncated functions $\bar{p}$, $\bar{q}$, and $\bar{r}$ can then be calculated. Actually, a more straightforward evaluation of the latter quantities can be made by using directly in the congruence procedure outlined above the scattering quantities $\bar{S}_{ij}$, $\bar{s}_{ij}$, and $\bar{\Delta}$ instead of S_{ij}, s_{ij}, and Δ in (18), (19), and (20). In this connection, notice that in the rather common case in which $\bar{s}_{12} = \text{const.}$ it is convenient to select for $\bar{r}$ the (constant) value $\bar{r}_{\text{opt}} = s'_{22,M}/(2\Delta'_M)$, which minimizes the degree of p and q.

Under transient operation, substitution of the operator $(\omega - \omega_o - jd/dt)$ for $(\omega - \omega_o)$ in the truncated counterpart of (13) finally provides the desired dynamic wafer-to-load transfer relationship:

$$V_L e^{j\Phi_L} = \sum_{0}^{P}{}_n \frac{(-j)^n}{n!}\frac{d^n\bar{p}}{d\omega^n}\frac{d^n(Ve^{j\phi})}{dt^n} + R_0\sum_{0}^{Q}{}_n \frac{(-j)^n}{n!}\frac{d^n\bar{q}}{d\omega^n}\frac{d^n(\bar{Y}_n Ve^{j\phi})}{dt^n} + \sum_{0}^{R}{}_n \frac{(-j)^n}{n!}\frac{d^n\bar{r}}{d\omega^n}\frac{d^n(Ee^{j\psi})}{dt^n}. \quad (21)$$

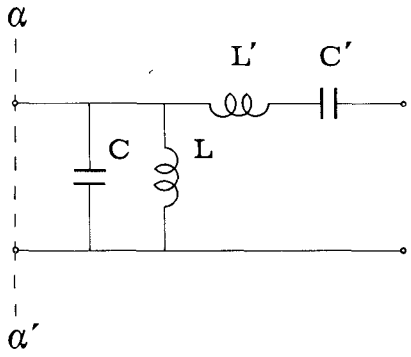

Fig. 3. Γ-type double-tuned tank and coupling circuit.

The above equation allows direct evaluation of the output voltage phasor in terms of the (known) input and of the (already calculated) wafer envelope components and their derivatives.

IV. Γ-Type Double-Tuned Oscillator

In order to illustrate the use of the method previously developed, we analyze here an injection-locked amplifier equipped with the (fourth-order, $M = 2$) tank and coupling circuit shown in Fig. 3. This ladder structure has been chosen both because it is the simplest one that enjoys the broad-banding properties discussed in [15] and because it does not lend itself to treatment by the other theories available in the literature.

For the sake of simplicity, we assume the nonlinear part of the diode admittance to be a quadratic function of the form

$$Y_n = (G_{n2} + j\omega C_{n2})V^2 \qquad (G_{n2} > 0) \quad (22)$$

and the two resonators to be synchronously tuned under free-running oscillation conditions ($V = V_o$, $\omega = \omega_o$)

$$L'C' = L(C + C_l + C_{n2}V_o^2) = 1/\omega_o^2 \quad (23)$$

which implies

$$V_o^2 = -\frac{1 + R_0G_l}{R_0G_{n2}}. \quad (24)$$

After introducing

$$\gamma = -R_0G_l \qquad Q = \frac{R_0}{\omega_o L}$$
$$Q' = \frac{\omega_o L'}{R_0} \qquad \omega_{or}^2 = \frac{1}{L(C + C_l)} \quad (25)$$

application of conversion formulas (A3) to the scattering

parameters of the augmented coupling two-port furnishes

$$s'_{11,0}=\frac{-\gamma}{QQ'} \qquad s''_{11,0}=\frac{-1}{\omega_o Q'}\left(1-\frac{\omega_o^2}{\omega_{or}^2}\right)$$

$$s'_{11,1}=\frac{1}{\omega_o^2}\left(1-\frac{\omega_o^2}{\omega_{or}^2}-\frac{\gamma}{QQ'}\right)$$

$$s''_{11,1}=\frac{1}{\omega_o^3}\left(\frac{\omega_o^2}{\omega_{or}^2 Q'}-\frac{\gamma+1}{Q}\right)$$

$$s'_{11,2}=\frac{-1}{\omega_o^2\omega_{or}^2}$$

$$s'_{12,0}=s'_{21,0}=\frac{-2}{QQ'}$$

$$s'_{12,1}=s'_{21,1}=\frac{-2}{\omega_o^2 QQ'}$$

$$s'_{22,0}=\frac{-\gamma}{QQ'} \qquad s''_{22,0}=\frac{-1}{\omega_o Q'}\left(1-\frac{\omega_o^2}{\omega_{or}^2}\right)$$

$$s'_{22,1}=\frac{-1}{\omega_o^2}\left(1-\frac{\omega_o^2}{\omega_{or}^2}+\frac{\gamma}{QQ'}\right)$$

$$s''_{22,1}=\frac{1}{\omega_o^3}\left(\frac{\omega_o^2}{\omega_{or}^2 Q'}+\frac{\gamma-1}{Q}\right)$$

$$s'_{22,2}=\frac{1}{\omega_o^2\omega_{or}^2}$$

$$\Delta'_0=\frac{\gamma-2}{QQ'} \qquad \Delta''_0=\frac{1}{\omega_o Q'}\left(1-\frac{\omega_o^2}{\omega_{or}^2}\right)$$

$$\Delta'_1=\frac{-1}{\omega_o^2}\left(1-\frac{\omega_o^2}{\omega_{or}^2}+\frac{2-\gamma}{QQ'}\right)$$

$$\Delta''_1=\frac{-1}{\omega_o^3}\left(\frac{\omega_o^2}{\omega_{or}^2 Q'}+\frac{1-\gamma}{Q}\right)$$

$$\Delta'_2=\frac{1}{\omega_o^2\omega_{or}^2}. \tag{26}$$

If we assume, as is reasonable, a small percent hot–cold detuning of the parallel resonator (i.e., $\omega_{or}\simeq\omega_o$) and high values for the quality factors Q and Q', the class defining conditions (9) are satisfied. A narrow-band approximation therefore provides the truncated scattering components

$$\bar{s}_{11}=-\left[\frac{\gamma}{QQ'}+\frac{j}{Q'}\left(1-\frac{\omega_o^2}{\omega_{or}^2}\right)\right]+\left[\frac{2}{\omega_o}\left(1-\frac{\omega_o^2}{\omega_{or}^2}\right)+j\frac{2}{\omega_o}\left(\frac{1}{Q'}-\frac{\gamma+1}{Q}\right)\right]\cdot(\omega-\omega_o)-\frac{4}{\omega_o^2}(\omega-\omega_o)^2$$

$$\bar{s}_{12}=\bar{s}_{21}=-\frac{2}{QQ'}$$

$$\bar{s}_{22}=-\left[\frac{\gamma}{QQ'}+\frac{j}{Q'}\left(1-\frac{\omega_o^2}{\omega_{or}^2}\right)\right]-\left[\frac{2}{\omega_o}\left(1-\frac{\omega_o^2}{\omega_{or}^2}\right)-j\frac{2}{\omega_o}\left(\frac{1}{Q'}+\frac{\gamma-1}{Q}\right)\right]\cdot(\omega-\omega_o)+\frac{4}{\omega_o^2}(\omega-\omega_o)^2$$

$$\bar{\Delta}=\left[\frac{\gamma-2}{QQ'}+\frac{j}{Q'}\left(1-\frac{\omega_o^2}{\omega_{or}^2}\right)\right]-\left[\frac{2}{\omega_o}\left(1-\frac{\omega_o^2}{\omega_{or}^2}\right)+j\frac{2}{\omega_o}\left(\frac{1}{Q'}-\frac{\gamma-1}{Q}\right)\right]\cdot(\omega-\omega_o)+\frac{4}{\omega_o^2}(\omega-\omega_o)^2 \tag{27}$$

where, as suggested in Section II, only significant terms (of magnitude order equal to $1/Q^{2-m}$ for $s^{(\cdot)}_{ij,m}$ and $\Delta^{(\cdot)}_m$, in this case) have been retained, thus avoiding unnecessary complication of the calculations. Making use of (27) in (11), after some algebra, we obtain the set of normalized differential equations

$$\frac{d^2X}{d\tau^2}=\left\{\gamma-\frac{1}{\eta}-3(\gamma-1)X^2\right\}\frac{dX}{d\tau}+\left\{2\nu+\beta(X^2-1)\right\}X\frac{d\phi}{d\tau}+X\left(\frac{d\phi}{d\tau}\right)^2+\left\{\nu^2+\left(\beta\nu-\frac{\gamma-1}{\eta}\right)(X^2-1)\right\}X+\frac{\rho}{\eta}\cos(\phi-\psi)$$

$$\frac{d^2\phi}{d\tau^2}=\left\{\beta(1-3X^2)-2\nu\right\}\frac{1}{X}\frac{dX}{d\tau}+\left\{\gamma-\frac{1}{\eta}-(\gamma-1)X^2\right\}\frac{d\phi}{d\tau}-\frac{2}{X}\frac{dX}{d\tau}\frac{d\phi}{d\tau}-\left\{\left(\frac{1}{\eta}-1\right)\nu+\left[(\gamma-1)\nu+\frac{\beta}{\eta}\right](X^2-1)\right\}-\frac{\rho}{\eta X}\sin(\phi-\psi) \tag{28}$$

in which

$$\eta=\frac{Q'}{Q} \qquad \beta=Q\left(1-\frac{\omega_o^2}{\omega_{or}^2}\right) \qquad X=\frac{V}{V_o}$$

$$\nu=2Q\left(\frac{\omega}{\omega_0}-1\right) \qquad \tau=\frac{\omega_o}{2Q}t \qquad \rho=\frac{E}{V_o}. \tag{29}$$

Notice in this connection that to comply with the assumption of a (unique) stable single-mode free-running oscillation at (V_o,ω_o), the following constraints on γ,η,β

$$\gamma>1 \qquad 4(1-\eta)(\gamma-1)^2-\eta^2\beta^2>0 \tag{30}$$

must be satisfied.

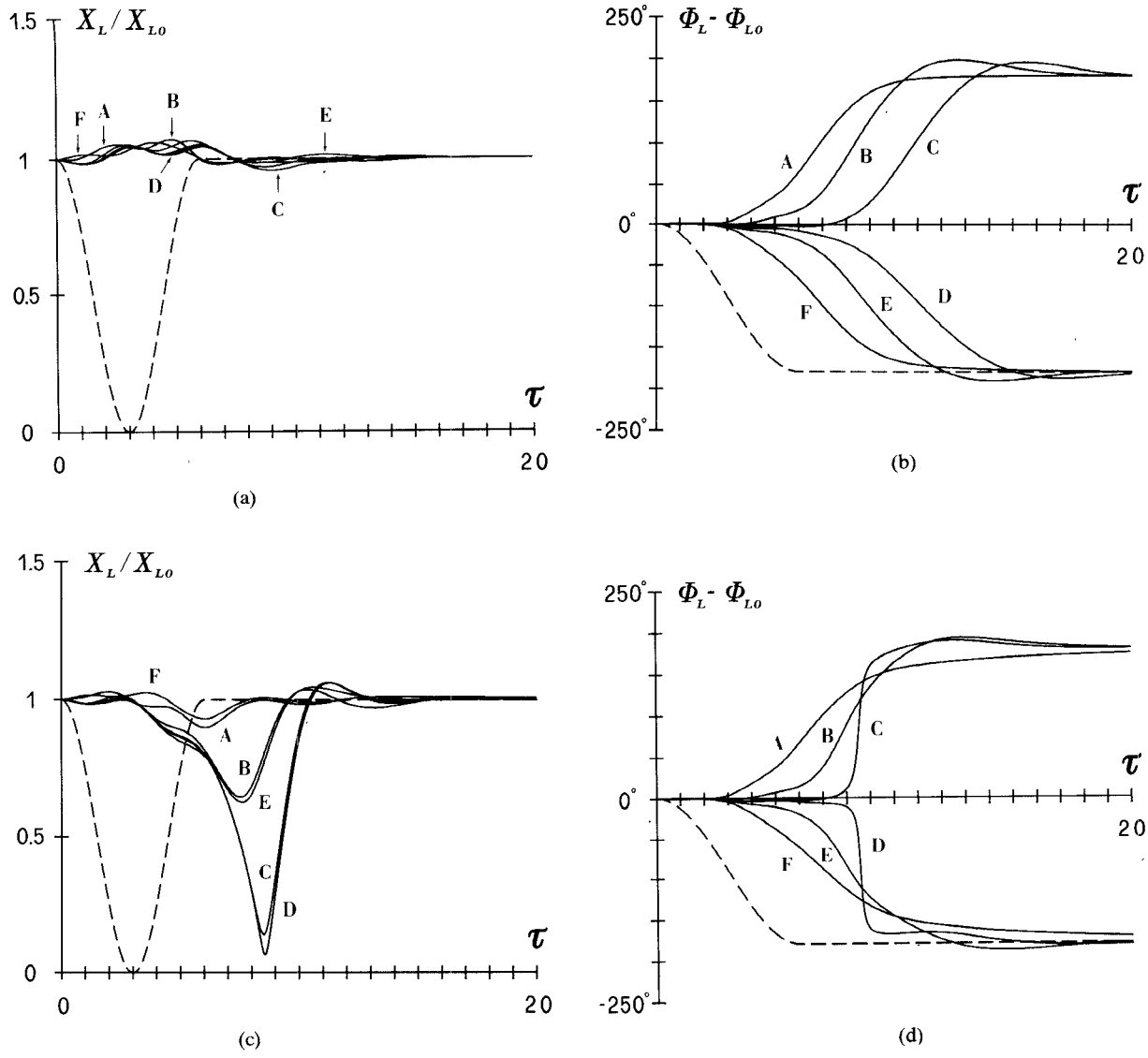

Fig. 4. Amplitude (a,c) and phase (b,d) transients of the output voltage scaled to relevant steady-state values (X_{LO}, ϕ_{LO}) before input signal switching. $\beta = 0$; $\eta = 0.75$; $\rho = -10$ dB; $\tau_s = 3$.
(a,b): $\gamma = 2$; $\nu = -0.6$(A), -0.3(B), -0.15(C), -0.10(D), 0(E), 0.6(F).
(c,d): $\gamma = 1.3$; $\nu = -0.6$(A), -0.3(B), -0.17(C), -0.15(D), 0(E), 0.6(F).
Dashed curves indicate (normalized) amplitude and phase evolution of the input signal.

As to the wafer-to-load dynamic transfer relationship, $\bar{s}_{12}$ being a constant, we choose for $\bar{r}$ the optimum value $\bar{r}_{opt} = 1/2$, thus obtaining $\bar{p} = \gamma + j(\beta - \nu)$, $\bar{q} = -1$. Use of such $\bar{p}, \bar{q}, \bar{r}$ in (21) and proper normalization yields finally

$$X_L = \left\{ k_1^2 + k_2^2 + \left[k_1 \cos(\phi - \psi) + k_2 \sin(\phi - \psi) \right] \rho + \frac{\rho^2}{4} \right\}^{1/2}$$

$$\phi_L = \psi + \tan^{-1} \left\{ \frac{k_1 \sin(\phi - \psi) - k_2 \cos(\phi - \psi)}{k_1 \cos(\phi + \psi) + \rho/2 + k_2 \sin(\phi - \psi)} \right\} \tag{31}$$

where

$$k_1 = -\frac{dX}{d\tau} + \left[1 + (1 - \gamma)(X^2 - 1) \right] X$$

$$k_2 = \left[\frac{d\phi}{d\tau} + \nu + \beta(X^2 - 1) \right] X. \tag{32}$$

V. Numerical Results for BPSK Modulation

Formulas derived in previous sections will be applied here to investigate, through computer simulation, the response of a Γ-type ILA to a binary (0°–±180°) phase shift keying modulated input signal. For brevity, only results concerning purely resistive nonlinearity ($\beta = 0$) will be reported here.

In order to better approximate the output waveform of a real-world BPSK modulator [13], the amplitude and the

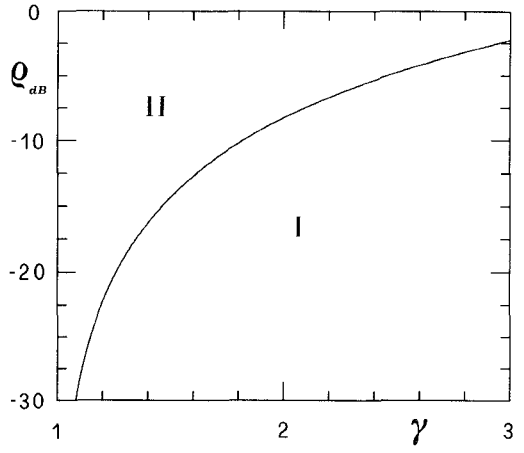

Fig. 5. Type I–type II threshold value of the injection power versus matching parameter (γ) for purely resistive nonlinearity ($\beta = 0$).

phase of the injection signal will be modeled as

$$\psi(\tau) = \begin{cases} 0, & \tau < 0 \\ \pm\dfrac{\pi}{2}\left(1-\cos\dfrac{\pi\tau}{2\tau_s}\right), & 0 \leqslant \tau \leqslant 2\tau_s \\ \pm\pi, & \tau > 2\tau_s \end{cases}$$

$$\rho(\tau) = \begin{cases} \rho, & \tau < 0 \\ \dfrac{\rho}{2}\left(1+\cos\dfrac{\pi\tau}{\tau_s}\right), & 0 \leqslant \tau \leqslant 2\tau_s \\ \rho, & \tau > 2\tau_s \end{cases} \qquad (33)$$

thus accounting for both a finite phase-switching time (τ_s) and an accompanying amplitude dip.

As far as the dynamics of the output waveform are concerned, behaviors of two (mutually exclusive) types have been observed when the carrier frequency is swept throughout the locking bandwidth, depending on the injection level and parameter values. Type I behavior is characterized by a set of transients (Fig. 4(a) and (b)) with a nearly constant amplitude and a smooth phase transition (from 0° to +180° or −180° depending on the carrier frequency) which becomes slower and slower as the injection frequency approaches a critical value, at which no phase reversal occurs. Type II behavior, instead, is characterized by a set of transients (Fig. 4(c) and (d)) with an ever-increasing dip in the amplitude and a steeper and steeper phase transition as the carrier frequency approaches the critical value, at which the voltage phasor vanishes, thus causing an abrupt 180° phase jump. Computed results indicate that the system behavior changes from type I to type II when the injection signal amplitude exceeds a threshold value, which monotonically increases with γ (see Fig. 5) and is independent of other circuit parameters.

The consequences of the above characteristics on the system performance as amplifier for BPSK modulated signals can be better illustrated by referring to the maximum switching time of the output phase (τ_x), defined as the maximum time required for the voltage out of a (balanced mixer) phase detector to cross the zero-threshold

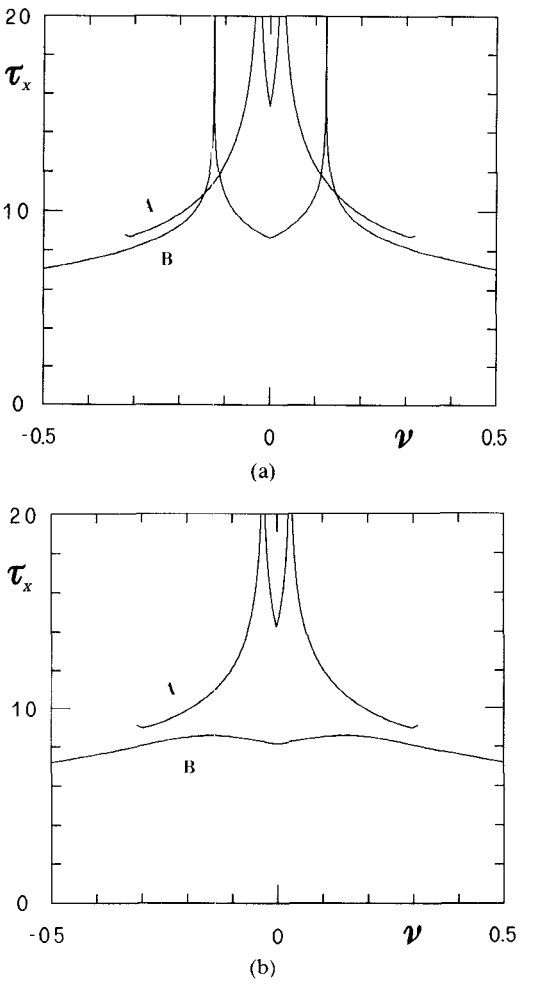

Fig. 6. Maximum output switching time versus input frequency offset. $\beta = 0$; $\eta = 0.75$; $\rho = -20$ dB(A), -10 dB(B); $\tau_s = 3$. (a) $\gamma = 2.0$; (b) $\gamma = 1.3$.

value when both a clockwise and a counterclockwise input phase transition are considered.

The dependence of τ_x on injection frequency and power is reported in Fig. 6, which clearly evidences that a case-by-case optimization of operating conditions is required in order to avoid critical dynamic responses. For instance, in the case of type I behavior (A, B curves of Fig. 6(a) and A curve of Fig. 6(b)), improper selection of the injection frequency with respect to the free-running oscillation one may cause switching times to be very long and/or markedly dependent on system parameter variations, because of the peaks appearing in the τ_x versus ν graphs. In this connection, observe that the most trivial choice of a synchronous injection ($\nu = 0$) is not satisfactory under small-signal operation (see A curves of Fig. 6). On the other hand, systems with type II responses show a nearly constant switching time within the locking band (e.g. B curve of Fig. 6(b)), and can therefore be optimized taking into consideration other performance indexes, such as the amplitude ripple.

Finally, as to the variation of τ_x with the input phase switching time τ_s, Figs. 7 and 8 evidence that while type II systems (A curves of Fig. 7 and curves of Fig. 8(b)) exhibit a smooth increase of τ_x with τ_s, when type I systems are

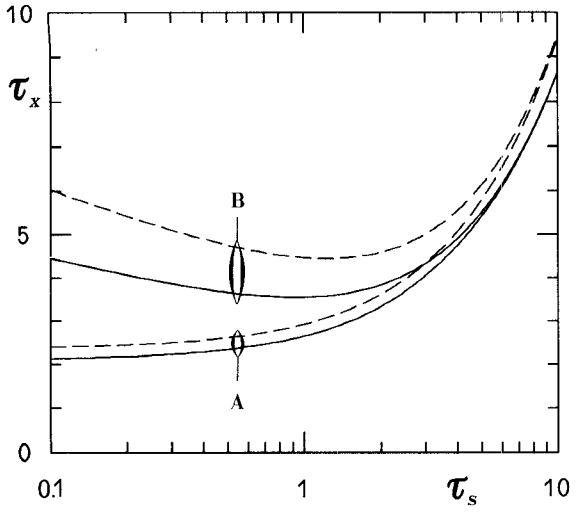

Fig. 7. Maximum output switching time versus input switching time. $\beta = 0$; $\gamma = 1.3$ (A), 2(B); $\eta = 0.25$ (-----), 0.75 (——); $\rho = -10$ dB; $\nu = 0$.

concerned (B curves of Fig. 7 and curves of Fig. 8(a)) an appropriate choice of τ_s (with respect to the other system parameters) has to be made in order to avoid an excessive increase of system response time.

VI. Conclusions

A method has been presented for the analysis of the transient behavior of high-order injection-locked amplifiers driven by modulated sinusoidal input signals which, in contrast to previous theories, also covers the case of large-signal injection operation.

The equivalent circuit considered includes an *RC* nonlinear element, modeling the negative resistance diode, and a linear lumped two-port described by its scattering matrix, modeling the tank and coupling structure, which permits the system identification to be performed directly in terms of measured data. Once ascertained, through a simple check on overall system parameters, that the basic constraints for quasi-sinusoidal quasi-static behavior are met, the two-step analysis procedure developed provides a pair of Mth-order differential equations in the amplitude and phase of the voltage at the wafer plane and a dynamical transfer relationship between wafer and load voltage phasors.

The performed computer simulation of a double-tuned oscillator driven by binary PSK input signal, showing a rather complex dependence of the system behavior on circuit parameters and operating conditions, evidences the importance of having at one's disposal accurate analysis tools for the design and optimization of injection-locked amplifiers with multiresonant tank and coupling structures.

Appendix I

Any function $W(j\omega)$ of the form

$$W(j\omega) = \sum_{0}^{M} w'_m \omega^{2m} + j\omega \sum_{0}^{M-1} w''_m \omega^{2m} \qquad \text{(A1)}$$

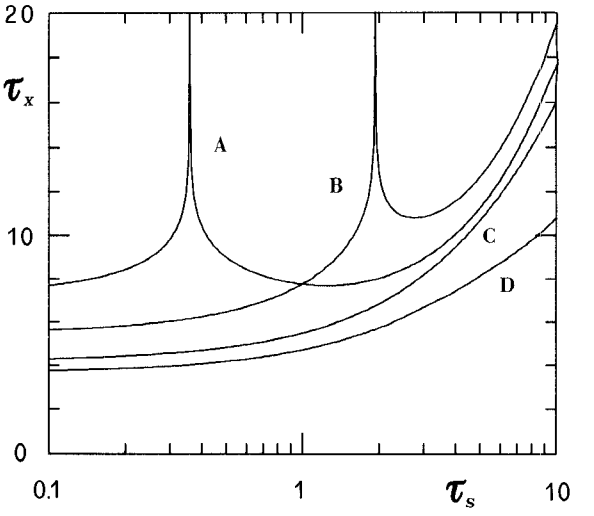

(a)

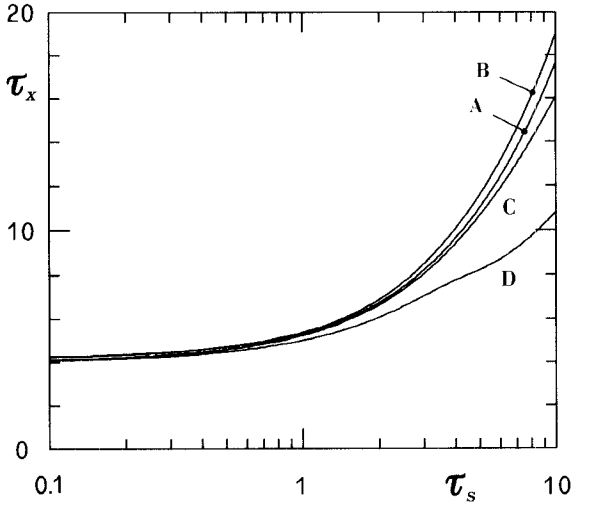

(b)

Fig. 8. Maximum output switching time versus input switching time. $\beta = 0$; $\eta = 0.75$; $\rho = -10$ dB; $\nu = 0.025$(A), 0.1(B), 0.3(C), 0.6(D); (a): $\gamma = 2.0$; (b): $\gamma = 1.3$

can be rearranged as

$$\sum_{0}^{M} {}_m \left(\omega^2 - \omega_o^2\right)^m \left(k'_m + j\omega k''_m\right) \qquad \text{(A2)}$$

with

$$k'_m = \sum_{0}^{M-m} {}_n \binom{m+n}{n} w'_{m+n} \omega_o^{2n} \qquad (m = 0, \cdots, M)$$

$$k''_m = \sum_{0}^{M-m-1} {}_n \binom{m+n}{n} w''_{m+n} \omega_o^{2n} \quad (m = 0, \cdots, M-1). \qquad \text{(A3)}$$

Indeed, letting

$$W(j\omega) = W'(\omega^2) + j\omega W''(\omega^2) \qquad \text{(A4)}$$

from (A2), by differentiation, we have

$$k_m^{(\cdot)} = \frac{1}{m!} \frac{d^m W^{(\cdot)}}{d(\omega^2)^m}\bigg|_{\omega = \omega_o} \qquad \text{(A5)}$$

while, from (A1), it is easily recognized that

$$\left.\frac{d^m W^{(\cdot)}}{d(\omega^2)^m}\right|_{\omega=\omega_o} = \sum_{0}^{M-m}{}_n \, w_{m+n}^{(\cdot)} \frac{(m+n)!}{n!}\omega_o^{2n}. \quad \text{(A6)}$$

Substitution of (A6) into (A5) demonstrates the assertion.

Appendix II

In order to evaluate the dynamical stability of the entrained oscillation, we linearize (12) in the neighborhoods of the equilibrium point (V_{eq}, ϕ_{eq}) setting there

$$V = V_{eq} + \Delta V \cdot e^{\lambda\tau} \qquad \phi = \phi_{eq} + \Delta\phi \cdot e^{\lambda\tau}. \quad \text{(A7)}$$

Resorting to matrix notation, we have therefore

$$\begin{bmatrix} \lambda^M - \sum_{0}^{M-1}{}_m \left.\frac{\partial f}{\partial x_m}\right|_{eq} \lambda^m & -\sum_{0}^{M-1}{}_m \left.\frac{\partial f}{\partial y_m}\right|_{eq} \lambda^m \\ -\sum_{0}^{M-1}{}_m \left.\frac{\partial g}{\partial x_m}\right|_{eq} \lambda^m & \lambda^M - \sum_{0}^{M-1}{}_m \left.\frac{\partial g}{\partial y_m}\right|_{eq} \lambda^m \end{bmatrix} \cdot \begin{bmatrix} \Delta V \\ \Delta\phi \end{bmatrix} = \mathbf{0} \quad \text{(A8)}$$

where, for conciseness, the following symbols have been introduced:

$$x_m = \frac{d^m V}{dt^m} \qquad y_m = \frac{d^m \phi}{dt^m} \quad \text{(A9)}$$

and the subscript "eq" indicates evaluation at $x_0 = V_{eq}$, $y_0 = \phi_{eq}$, $x_m = y_m = 0$ $(m = 1, 2, \cdots, M-1)$. From (A8) we get finally the characteristic equation

$$\begin{aligned} &\lambda^{2M} - \left[\frac{\partial f}{\partial x_{M-1}} + \frac{\partial g}{\partial y_{M-1}}\right]_{eq} \lambda^{2M-1} \\ &- \sum_{M}^{2M-2}{}_m \left[\frac{\partial f}{\partial x_{m-M}} + \frac{\partial g}{\partial y_{m-M}} \right. \\ &\left. - \sum_{m-M+1}^{M-1}{}_n \left(\frac{\partial f}{\partial x_n}\frac{\partial g}{\partial y_{m-n}} - \frac{\partial f}{\partial y_{m-n}}\frac{\partial g}{\partial x_n}\right)\right]_{eq} \lambda^m \\ &+ \sum_{0}^{M-1}{}_m \left[\sum_{0}^{m}{}_n \left(\frac{\partial f}{\partial x_n}\frac{\partial g}{\partial y_{m-n}} - \frac{\partial f}{\partial y_{m-n}}\frac{\partial g}{\partial x_n}\right)\right]_{eq} \lambda^m = 0. \end{aligned} \quad \text{(A10)}$$

Appendix III

For the reader's convenience, some basic properties of polynomial congruences are reported here.

If a polynomial $p_0(x)$ divides the difference of two other polynomials $p_1(x)$ and $p_2(x)$ by a factor $h(x)$, i.e., if

$$p_1(x) - p_2(x) = h(x) \cdot p_0(x) \quad \text{(A11)}$$

then $p_1(x)$ is said to be congruent to $p_2(x)$ modulo $p_0(x)$, which is written as

$$p_1(x) \equiv p_2(x) \qquad [\text{mod } p_0(x)]. \quad \text{(A12)}$$

Solving a congruence of the form

$$p_1(x) \cdot r(x) \equiv p_2(x) \qquad [\text{mod } p_0(x)] \quad \text{(A13)}$$

with $p_i(x)$ assigned polynomials, means to determine the polynomial sets $\{r(x)\}$ which "satisfy" (A13) in the sense specified above. In this connection, let us observe that if $r_0(x)$ is a minimum degree solution (i.e., of degree lesser than the modulus), the polynomials $r(x) = r_0(x) + n(x)p_0(x)$ (for any $n(x)$) will constitute a set of solutions of (A13). Generally speaking, a congruence may be solvable or not. However, as previously pointed out, circuit theory ensures that the congruences of Section III are always solvable, of which circumstance account will be taken in the sequel. Further, only minimum degree solutions will be considered here. In the trivial case where $p_0(x)$ is a zeroth-degree polynomial, an arbitrary constant value can be chosen for r_0. In the general case, a congruence of the form (A13) can be solved resorting to a recursive algorithm whose ith cycle consists of the following three steps:

1) Replace the ith congruence

$$p_1^{(i)} r^{(i)} \equiv p_2^{(i)} \qquad [\text{mod } p_0^{(i)}] \quad \text{(A14)}$$

with the equivalent congruence

$$q_1^{(i)} \cdot r^{(i)} \equiv q_2^{(i)} \qquad [\text{mod } p_0^{(i)}] \quad \text{(A15)}$$

where $q_j^{(i)}$ is the rest of the division $p_j^{(i)}/p_0^{(i)}$.

2) Replace the congruence (A15) with the reduced congruence

$$p_0^{(i)} \cdot r^{(i+1)} \equiv -q_2^{(i)} \qquad [\text{mod } q_1^{(i)}] \quad \text{(A16)}$$

whose solution $(r^{(i+1)})$ is related to the solution of (A15) through the relationship

$$r^{(i)} \equiv \frac{p_0^{(i)} \cdot r^{(i+1)} + q_2^{(i)}}{q_1^{(i)}}. \quad \text{(A17)}$$

3) Increment index i to $i+1$ setting

$$\begin{aligned} p_1^{(i+1)} &= p_0^{(i)} \\ p_2^{(i+1)} &= q_2^{(i)} \\ p_0^{(i+1)} &= q_1^{(i)} \end{aligned} \quad \text{(A18)}$$

and go back to step 1).

This way, at every cycle the degree of the modulus is lowered. The procedure stops when the modulus becomes a first-degree polynomial, viz. when

$$C_1 \cdot r^{(I)} \equiv C_2 \qquad [\text{mod } (C_{00} + C_{01} \cdot x)] \quad \text{with} \quad C_{(\ )} = \text{const.} \quad \text{(A19)}$$

from which one obtains $r^{(I)} = C_2/C_1$. Repeated application of formula (A17) eventually furnishes $r^{(1)}$.

References

[1] T. Isobe and M. Tokida, "Power amplification for FM and PM signals with synchronized IMPATT oscillators," *IEEE Trans. Microwave Theory Tech.*, vol MTT-18, pp. 906–911, Nov. 1970.

[2] Y Takayama, "Power amplification with IMPATT diodes in stable and injection-locked modes," *IEEE Trans. Microwave Theory Tech.*, vol MTT-20, pp. 266–272, Apr. 1972.

[3] J J. Goedbloed and M. T. Vlaardingerbroek, "Theory of noise and transfer properties of IMPATT diode amplifiers," *IEEE Trans. Microwave Theory Tech*, vol MTT-25, pp. 324–332, Apr 1977.

[4] B. N. Biswas, S. K. Ray, K. Pramanik, M. Sadhu and D. Bandyopadhyay, "Hold-in characteristics of an extended range Gunn oscillator system," *IEEE Trans. Microwave Theory Tech.*, vol. MTT-31, pp. 271–276, Mar. 1983.
[5] D. H. Evans and R. N. Bates, "Novel 93 GHz injection-locked IMPATT oscillator," *Electron. Lett.*, vol. 23, pp. 771–772, July 1987.
[6] B. van der Pol, "Forced oscillations in a circuit with non-linear resistance," *Phil. Mag.*, vol. S.7, vol. 3, pp. 65–80, Jan. 1927.
[7] R. Adler, "A study of locking phenomena in oscillators," *Proc. IRE*, vol. 34, pp. 351–357, June 1946; reprinted in *Proc. IEEE*, vol. 61, pp. 1380–1385, Oct. 1973.
[8] L. J. Paciorek, "Injection locking of oscillators," *Proc. IEEE*, vol. 53, pp. 1723–1727, Nov. 1965.
[9] H. L. Stover and R. C. Shaw, "Injection-locked oscillators and amplifiers for angle modulated signals," in *1966 IEEE MTT-S Int. Microwave Symp. Dig.*, (Palo Alto, CA), May 16–19, 1966, pp. 60–65.
[10] T. L. Osborne, "Amplitude behavior of injection-locked oscillators," *IEEE Trans. Microwave Theory Tech.*, vol. MTT-18, pp. 897–905, Nov. 1970.
[11] K. Daikoku and Y. Mizushima, "Properties of injection locking in the non-linear oscillator," *Int. J. Electron.*, vol. 31, pp. 279–292, Mar. 1971.
[12] J. Nigrin, P. A. Goud, and J. F. W. Gurke, "Distortion of FM modulation in injection phase-locked oscillator-amplifiers," *Proc. IEEE*, vol. 60, pp. 731–732, June 1972.
[13] H. J. Kuno, "Analysis of nonlinear characteristics and transient response of IMPATT amplifiers," *IEEE Trans. Microwave Theory Tech.*, vol. MTT-21, pp. 694–702, Nov. 1973.
[14] D. Pavlidis, H. L. Hartnagel and K. Tomizawa, "Dynamic considerations of injection locked pulsed oscillators with very fast switching characteristics," *IEEE Trans. Microwave Theory Tech.*, vol. MTT-26, pp. 162–169, Mar. 1978.
[15] K. Kurokawa, "Some basic characteristics of broadband negative resistance oscillator circuits," *Bell Syst. Tech. J.*, vol. 48, pp. 1937–1955, July–Aug. 1969.
[16] Y. Takayama, "Dynamic behavior of nonlinear power amplifiers in stable and injection-locked modes," *IEEE Trans. Microwave Theory Tech.*, vol. MTT-20, pp. 591–595, Sept. 1972.
[17] K. Kurokawa, "Injection locking of microwave solid-state oscillators," *Proc. IEEE*, vol. 61, pp. 1386–1410, Oct. 1973.
[18] M. Nakajima and J. Ikenoue, "Locking phenomena in microwave oscillators," *Int. J. Electron.*, vol. 44, pp. 465–472, May 1978.
[19] K. Kurokawa, "Stability of injection-locked oscillators," *Proc. IEEE*, vol. 60, pp. 907–908, July 1972.
[20] E. F. Calandra and A. M. Sommariva, "Stability analysis of injection-locked oscillators in their fundamental mode of operation," *IEEE Trans. Microwave Theory Tech.*, vol. MTT-29, pp. 1137–1144, Nov. 1981.
[21] B. A. Syrett, "Computer-aided large-signal measurement of IMPATT-diode electronic admittance," *IEEE Trans. Microwave Theory Tech.*, vol. MTT-27, pp. 830–834, Oct. 1979.
[22] H. J. Pauwels, "First harmonic approximation in nonlinear filtered circuits," *Proc. IEEE*, vol. 55, pp. 1744–1745, Oct. 1967.
[23] E. F. Calandra and A. M. Sommariva, "On the dynamical stability of negative conductance free-running oscillators," *Proc. Inst. Elec. Eng.*, vol. 132, pt. G, pp. 143–148, Aug. 1985.
[24] N. Minorsky, *Nonlinear Oscillations*. Princeton, N.J.: Van Nostrand, 1962.
[25] I. Niven and H. S. Zuckerman, *An Introduction to the Theory of Numbers*. New York: Wiley, 1980.

✠

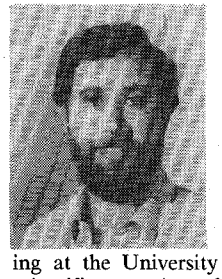

Enrico F. Calandra (S'76–M'78) was born in Messina, Italy. He received the "Laurea in Ingegneria Elettronica" from the University of Palermo, Italy, in 1978.

From 1978 to 1983, he was a member of the Research Staff of the Microwave Department of the Centro per la Ricerca Elettronica in Sicilia (CRES), Monreale, Italy, where he was engaged in the development of coherent MTI radar systems. Since 1983, he has been an Assistant Professor in the Department of Electrical Engineering at the University of Palermo, Italy. Since 1985 he has also been scientific supervisor of the Microwave Department of CRES. His research interests are in the fields of nonlinear circuits and low-noise techniques and measurements.

✠

Antonino M. Sommariva was born in Palermo, Italy. He received the "Laurea in Ingegneria Elettronica" from the University of Palermo, Italy, in 1977.

Thereafter, he joined the Centro per la Ricerca Elettronica in Sicilia (CRES), Monreale, Italy, where in 1979 he was appointed Head of the Microwave Department. Since 1983, he has been an Assistant Professor in the Department of Electrical Engineering of the University of Palermo, Italy. His research interests are focused on the theory of nonlinear oscillations in electrical circuits.